

A statistical approach to the traceroute-like exploration of networks: theory and simulations

Luca Dall'Asta, Ignacio Alvarez-Hamelin, Alain Barrat, Alexei Vázquez, Alessandro Vespignani

Abstract— Mapping the Internet generally consists in sampling the network from a limited set of sources by using traceroute-like probes. This methodology, akin to the merging of different spanning trees to a set of destinations, has been argued to introduce uncontrolled sampling biases that might produce statistical properties of the sampled graph which sharply differ from the original ones [7–9]. Here we explore these biases and provide a statistical analysis of their origin. We derive a mean-field analytical approximation for the probability of edge and vertex detection that exploits the role of the number of sources and targets and allows us to relate the global topological properties of the underlying network with the statistical accuracy of the sampled graph. In particular we find that the edge and vertex detection probability is depending on the *betweenness centrality* of each element. This allows us to show that shortest path routed sampling provides a better characterization of underlying graphs with scale-free topology. We complement the analytical discussion with a throughout numerical investigation of simulated mapping strategies in different network models. We show that sampled graphs provide a fair qualitative characterization of the statistical properties of the original networks in a fair range of different strategies and exploration parameters. The numerical study also allows the identification of intervals of the exploration parameters that optimize the fraction of nodes and edges discovered in the sampled graph. This finding might hint the steps toward more efficient mapping strategies.

Keywords—Traceroute, Internet exploration, Topology inference.

I. INTRODUCTION

A significant research and technical challenge in the study of large information networks is related to the lack of highly accurate maps providing information on their basic topology. This is mainly due to the dynamical nature of their structure and to the lack of any centralized con-

L. Dall'Asta, I. Alvarez-Hamelin, A. Barrat, A. Vespignani are with L.P.T., Bâtiment 210, Université de Paris-Sud, 91405 ORSAY Cedex France.

A. Vázquez is with Department of Physics, University of Notre Dame, Notre Dame, IN 46556, USA.

I. Alvarez-Hamelin is also with Facultad de Ingeniería, Universidad de Buenos Aires, Paseo Colón 850, C 1063 ACV Buenos Aires, Argentina.

A. Vespignani is also with School of Informatics and Department of Physics, University of Indiana, Bloomington, IN 47408, USA.

trol resulting in a self-organized growth and evolution of these systems. A prototypical example of this situation is faced in the case of the physical Internet. The topology of the Internet can be investigated at different granularity levels such as the router and Autonomous System (AS) level, with the final aim of obtaining an abstract representation where the set of routers or ASs and their physical connections (peering relations) are the vertices and edges of a graph, respectively. In the absence of accurate maps, researchers rely on a general strategy that consists in acquiring local views of the network from several vantage points and merging these views in order to get a presumably accurate global map. Local views are obtained by evaluating a certain number of paths to different destinations by using specific tools such as traceroute or by the analysis of BGP tables. At first approximation these processes amount to the collection of shortest paths from a source node to a set of target nodes, obtaining a partial spanning tree of the network. The merging of several of these views provides the map of the Internet from which the statistical properties of the network are evaluated.

By using this strategy a number of research groups have generated maps of the Internet [1–5], that have been used for the statistical characterization of the network properties. Defining $\mathcal{G} = (V, E)$ as the sampled graph of the Internet with $N = |V|$ vertices and $|E|$ edges, it is quite intuitive that the Internet is a *sparse* graph in which the number of edges is much lower than in a complete graph; i.e. $|E| \ll N(N - 1)/2$. Equally important is the fact that the average distance, measured as the shortest path, between vertices is very small. This is the so called *small-world* property, that is essential for the efficient functioning of the network. Most surprising is the evidence of a power-law relationship between the frequency of vertices and their degree k defined as the number of edges linking each vertex to its neighbors. Namely, the probability that any vertex in the graph has degree k is well approximated by $P(k) \sim k^{-\gamma}$ with $2 \leq \gamma \leq 2.5$ [6]. Evidence for the heavy-tailed behavior of the degree distribution has been collected in several other studies at the router and AS level [10–14] and have generated a large activity in the field of network modeling and characterization [15–19].

While traceroute-driven strategies are very flexi-

ble and can be feasible for extensive use, the obtained maps are undoubtedly incomplete. Along with technical problems such as the instability of paths between routers and interface resolutions [20], typical mapping projects are run from relatively small sets of sources whose combined views are missing a considerable number of edges and vertices [14, 21]. In particular, the various spanning trees are specially missing the lateral connectivity of targets and sample more frequently nodes and links which are closer to each source, introducing spurious effects that might seriously compromise the statistical accuracy of the sampled graph. These *sampling biases* have been explored in numerical experiments of synthetic graphs generated by different algorithms [7–9]. Very interestingly, it has been shown that apparent degree distributions with heavy-tails may be observed even from regular topologies such as in the classic Erdős-Rényi graph model [7, 8]. These studies thus point out that the evidence obtained from the analysis of the Internet sampled graphs might be insufficient to draw conclusions on the topology of the actual Internet network.

In this work we tackle this problem by performing a mean-field statistical analysis and extensive numerical experiments of shortest path routed sampling in different networks models. We find an approximate expression for the probability of edges and vertices to be detected that exploits the dependence upon the number of sources, targets and the topological properties of the networks. This expression allows the understanding of the qualitative behavior of the efficiency of the exploration methods by changing the number of probes imposed to the graph. Moreover, the analytical study provides a general understanding of which kind of topologies yields the most accurate sampling. In particular, we show that the map accuracy depends on the underlying network *betweenness centrality* distribution; the broader the distribution the higher the statistical accuracy of the sampled graph.

We substantiate our analytical finding with a throughout analysis of maps obtained varying the number of source-target pairs on networks models with different topological properties. The results show that single source mapping processes face serious limitations in that also the targeting of the whole network results in a very partial discovery of its connectivity. On the contrary, the use of multiple sources promptly leads to a consistent increase in the accuracy of the obtained maps where the statistical degree distributions are qualitatively discriminated also at low values of target density. A detailed discussion of the behavior of the degree distribution and other statistical quantities as a function of target and sources is provided for sampled graphs with different topologies and compared with the in-

sight obtained by analytical means.

We also inspect quantitatively the portion of discovered network in different mapping process imposing the same density of probes to the network. We find the presence of a region of low efficiency (less nodes and edges discovered) depending on the relative proportion of sources and targets. Furthermore, the analysis of the optimal range of sources and targets for the estimate of the network average degree and clustering indicates a different parameters region. This finding calls for a “trade-off” between the accuracy in the observation of different quantities and hints to possible optimization procedures in the traceroute-driven mapping of large networks.

II. RELATED WORK

A certain number of works have been devoted to the study of sampled graphs obtained by shortest path probing procedures, and to the assessment of their accuracy. We present a short survey of the works which are related to ours.

Work by Lakhina et al. [7] has shown that power-law like distributions can be obtained for subgraphs of Erdős-Rényi random graphs when the subgraph is the result of a traceroute exploration with relatively few sources and destinations. They discuss the origin of these biases and the effect of the distance between source and target in the mapping process.

In a recent work [8], Clauset and Moore have studied analytically the single source probing to all possible destinations of an Erdős-Renyi random graph with average degree \bar{k} . In agreement with the numerical study of Lakhina et al. [7] they have found that the connectivity distribution of the obtained spanning tree displays a power-law behavior k^{-1} , with an exponential cut-off setting in at a characteristic degree $k_c \sim \bar{k}$.

In Ref. [9], Petermann and De Los Rios have studied a traceroute-like procedure on various examples of scale-free graphs, showing that, in the case of a single source, power-law distributions with underestimated exponents are obtained. Analytical estimates of the measured exponents as a function of the true ones were also derived. Finally, in a recent preprint appeared during the completion of our work, Guillaume and Latapy [23] report about the shortest-paths explorations of synthetic graphs, comparing properties of the resulting sampled graph with those of the original network. The exploration is made using level plots for the proportion of discovered nodes and edges in the graph as a function of the number of sources and targets, giving also hints for optimal placement of sources and targets. All these pieces of work make clear the relevance of determining up to which extent the

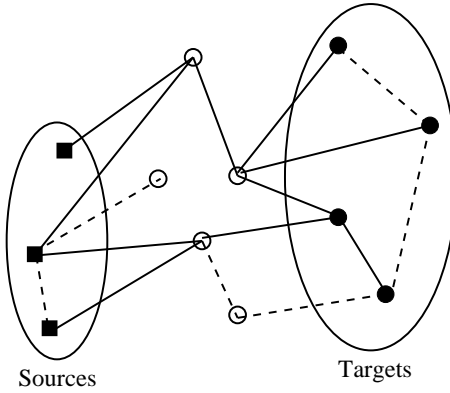


Fig. 1

ILLUSTRATION OF THE TRACEROUTE-LIKE PROCEDURE. SHORTEST PATHS BETWEEN THE SET OF SOURCES AND THE SET OF DESTINATION TARGETS ARE DISCOVERED (SHOWN IN FULL LINES) WHILE OTHER EDGES ARE NOT FOUND (DASHED LINES). NOTE THAT NOT ALL SHORTEST PATHS ARE FOUND SINCE THE “UNIQUE SHORTEST PATH” PROCEDURE IS USED.

topological properties observed in sampled graphs are representative of that of the real networks.

III. MODELING THE TRACEROUTE DISCOVERY OF UNKNOWN NETWORKS

In a typical traceroute study, a set of active sources deployed in the network run traceroute probes to a set of destination nodes. Each probe collects information on all the nodes and edges traversed along the path connecting the source to the destination, allowing the discovery of the network [20]. By merging the information collected on each path it is then possible to reconstruct a partial map of the network (see Fig.1). More in detail, the edges and the nodes discovered by each probe will depend on the metric \mathcal{M} used to decide the path between a pair of nodes. While in the Internet many factors, including commercial agreement and administrative routing policies, contribute to determine the actual path, it is clear that to a first approximation the route obtained by traceroute-like probes is the shortest path between the two nodes. This assumption, however, is not sufficient for a proper definition of a traceroute model in that equivalent shortest paths between two nodes may exist. In the presence of a degeneracy of shortest paths we must therefore specify the metric \mathcal{M} by providing a resolution algorithm for the selection of shortest paths.

For the sake of simplicity we can define three selection mechanisms defining different \mathcal{M} -paths that may account for some of the features encountered in Internet discovery:

- Unique Shortest Path (USP) probe. In this case the shortest path route selected between a node i and the destination target T is always the same independently of the source S (the path being initially chosen at random among all the equivalent ones).
- Random Shortest Path (RSP) probe. The shortest path between any source-destination pair is chosen randomly among the set of equivalent shortest paths. This might mimic different peering agreements that make independent the paths among couples of nodes.
- All Shortest Paths (ASP) probe. The metric discovers all the equivalent shortest paths between source-destination pairs. This might happen in the case of probing repeated in time (long time exploration), so that back-up paths and equivalent paths are discovered in different runs.

Actual traceroute probes contain a mixture of the three mechanisms defined above. We do not attempt, however, to account for all the subtleties that real studies encounters, i.e. IP routing, BGP policies, interface resolutions and many others. Each traceroute probe provides a test of the possible biases and we will see that the different metrics have only little influence on the general picture emerging from our results. On the other hand, it is intuitive to recognize that the USP metric represents the worst case scenario since, among the three different methods, it yields the minimum number of discoveries. For this reason, if not otherwise specified, we will report the USP data to illustrate the general features of our synthetic exploration.

More formally, the experimental setup for our simulated traceroute mapping is the following. Let $G = (V, E)$ be a sparse undirected graph with vertices (nodes) $V = \{1, 2, \dots, N\}$ and edges (links) $E = \{i, j\}$. Then let us define the sets of vertices $\mathcal{S} = \{i_1, i_2, \dots, i_{N_S}\}$ and $\mathcal{T} = \{j_1, j_2, \dots, j_{N_T}\}$ specifying the random placement of N_S sources and N_T destination targets. For each ensemble of source-target pairs $\Omega = \{\mathcal{S}, \mathcal{T}\}$, we compute with the metric \mathcal{M} the path connecting each source-target pair. The sampled graph $\mathcal{G} = (V^*, E^*)$ is defined as the set of vertices V^* (with $N^* = |V^*|$) and edges E^* induced by considering the union of all the \mathcal{M} -paths connecting the source-target pairs. The sampled graph is thus analogous to the maps obtained from real traceroute sampling of the Internet.

In our study the parameters of interest are the density $\rho_T = N_T/N$ and $\rho_S = N_S/N$ of targets and sources. In general, traceroute-driven studies run from a relatively small number of sources to a much larger set of destinations. For this reason, in many cases it is appropriate to work with the density of targets ρ_T while still considering N_S instead of the corresponding density. Indeed, it is

clear that while 100 targets may represent a fair probing of a network composed by 500 nodes, this number would be clearly inadequate in a network of 10^6 nodes. On the contrary, the density of targets ρ_T allows us to compare mapping processes on networks with different sizes by defining an intrinsic percentage of targeted vertices. In many cases, as we will see in the next sections, an appropriate quantity representing the level of sampling of the networks is

$$\epsilon = \frac{N_S N_T}{N} = \rho_T N_S, \quad (1)$$

that measures the density of probes imposed to the system. In real situations it represents the density of traceroute probes in the network and therefore a measure of the load provided to the network by the measuring infrastructure.

In the following, our aim is to evaluate to which extent the statistical properties of the sampled graph \mathcal{G} depend on the parameters of our experimental setup and are representative of the properties of the underlying graph G .

IV. MEAN-FIELD THEORY OF THE DISCOVERY BIAS

We begin our study by presenting a mean-field statistical analysis of the simulated traceroute mapping. Our aim is to provide a statistical estimate for the probability of edge and node detection as a function of N_S , N_T and the topology of the underlying graph.

For each set $\Omega = \{\mathcal{S}, \mathcal{T}\}$ we can define the quantities

$$\sum_{t=1}^{N_T} \delta_{i,j_t} = \begin{cases} 1 & \text{if vertex } i \text{ is a target;} \\ 0 & \text{otherwise,} \end{cases} \quad (2)$$

$$\sum_{s=1}^{N_S} \delta_{i,i_s} = \begin{cases} 1 & \text{if vertex } i \text{ is a source;} \\ 0 & \text{otherwise,} \end{cases} \quad (3)$$

where $\delta_{i,j}$ is the Kronecker symbol. These quantities tell us if any given node i belongs to the set of sources or targets, and obey the sum rules $\sum_i \sum_{t=1}^{N_T} \delta_{i,j_t} = N_T$ and $\sum_i \sum_{s=1}^{N_S} \delta_{i,i_s} = N_S$. Analogously, we define the quantity $\sigma_{i,j}^{(l,m)}$ that assumes the value 1 if the edge (i, j) belongs to the \mathcal{M} -path between nodes l and m , and 0 otherwise. By using the above definitions, the probability that a given edge (i, j) will be discovered and belongs to the sampled graph is given by

$$\pi_{i,j} = 1 - \prod_{l \neq m} \left(1 - \sum_{s=1}^{N_S} \delta_{l,i_s} \sum_{t=1}^{N_T} \delta_{m,j_t} \sigma_{i,j}^{(l,m)} \right). \quad (4)$$

In the case of a given set $\Omega = \{\mathcal{S}, \mathcal{T}\}$, the discovery probability is simply $\pi_{i,j} = 1$ if the edge (i, j) belongs to at least one of the \mathcal{M} -paths connecting the source-target pairs, and 0 otherwise. While the above exact expression

does not lead us too far in the understanding of the discovery probabilities, it is interesting to look at the process on a statistical ground by studying the average over all possible realizations of the set $\Omega = \{\mathcal{S}, \mathcal{T}\}$. By definition we have that

$$\left\langle \sum_{t=1}^{N_T} \delta_{i,j_t} \right\rangle = \rho_T \quad \text{and} \quad \left\langle \sum_{s=1}^{N_S} \delta_{i,i_s} \right\rangle = \rho_S, \quad (5)$$

where $\langle \dots \rangle$ identifies the average over all possible deployment of sources and targets Ω . These equalities simply state that each node i has, on average, a probability to be a source or a target that is proportional to their respective densities. In the following, we will make use of an uncorrelation assumption that allows an explicit approximation for the discovery probability. The assumption consists in neglecting correlations originated by the position of sources and targets on the discovery probability by different paths. While this assumption does not provide an exact treatment for the problem it generally conveys a qualitative understanding of the statistical properties of the system. In this approximation, the average discovery probability of an edge is

$$\begin{aligned} \langle \pi_{i,j} \rangle &= 1 - \left\langle \prod_{l \neq m} \left(1 - \sum_{s=1}^{N_S} \delta_{l,i_s} \sum_{t=1}^{N_T} \delta_{m,j_t} \sigma_{i,j}^{(l,m)} \right) \right\rangle \\ &\simeq 1 - \prod_{l \neq m} \left(1 - \rho_T \rho_S \langle \sigma_{i,j}^{(l,m)} \rangle \right), \end{aligned} \quad (6)$$

where in the last term we take advantage of neglecting correlations by replacing the average of the product of variables with the product of the averages and using Eq. (5). This expression simply states that each possible source-target pair weights in the average with the product of the probability that the end nodes are a source and a target; the discovery probability is thus obtained by considering the edge in an average effective medium (*mean-field*) of sources and targets homogeneously distributed in the network. This approach is indeed akin to mean-field methods customarily used in the study of many particle systems where each particle is considered in an effective average medium defined by the uncorrelated averages of quantities. The realization average of $\langle \sigma_{i,j}^{(l,m)} \rangle$ is very simple in the uncorrelated picture, depending only of the kind of \mathcal{M} -path. In the case of the ASP probing we have $\langle \sigma_{i,j}^{(l,m)} \rangle = \sigma_{i,j}^{(l,m)}$, in that each path contributes to the discovery of the edge. In the case of the USP and the RSP, however, only one path among all the equivalent ones is chosen, and in the average we have that each shortest path gives a contribution $\sigma_{i,j}^{(l,m)} / \sigma^{(l,m)}$ to $\langle \sigma_{i,j}^{(l,m)} \rangle$, where

$\sigma^{(l,m)}$ is the number of equivalent shortest path between vertices l and m .

The standard situation we consider is the one in which $\rho_T \rho_S \ll 1$ and since $\langle \sigma_{i,j}^{(l,m)} \rangle \leq 1$, we have

$$\prod_{l \neq m} \left(1 - \rho_T \rho_S \langle \sigma_{i,j}^{(l,m)} \rangle\right) \simeq \prod_{l \neq m} \exp \left(-\rho_T \rho_S \langle \sigma_{i,j}^{(l,m)} \rangle\right), \quad (7)$$

that inserted in Eq.(6) yields

$$\begin{aligned} \langle \pi_{i,j} \rangle &\simeq 1 - \prod_{l \neq m} \left(\exp \left(-\rho_T \rho_S \langle \sigma_{i,j}^{(l,m)} \rangle\right) \right) \\ &= 1 - \exp(-\rho_T \rho_S b_{ij}), \end{aligned} \quad (8)$$

where $b_{ij} = \sum_{l \neq m} \langle \sigma_{i,j}^{(l,m)} \rangle$. In the case of the USP and RSP probing, the quantity b_{ij} is by definition the edge betweenness centrality [24, 25], sometimes also referred to as “load” [26] (In the case of ASP probing, it is a closely related quantity). Indeed the vertex or edge betweenness is defined as the total number of shortest paths among pairs of vertices in the network that pass through a vertex or an edge, respectively. If there are multiple shortest paths between a pair of vertices, the path contributes to the betweenness with the corresponding relative weight. The betweenness gives a measure of the amount of all-to-all traffic that goes through an edge or vertex, if the shortest path is used as the metric defining the optimal path between pairs of vertices, and it can be considered as a non-local measure of the *centrality* of an edge or vertex in the graph.

The edge betweenness assumes values between 2 and $N(N-1)$ and the discovery probability of the edge will therefore depend strongly on its betweenness. In particular, for vertices with minimum betweenness $b_{ij} = 2$ we have

$$\langle \pi_{i,j} \rangle \simeq 2\rho_T \rho_S, \quad (9)$$

that recovers the probability that the two end vertices of the edge are chosen as source and target. This implies that if the densities of sources and targets are small but finite in the limit of very large N , all the edges in the underlying graph have an appreciable probability to be discovered. Moreover, for a large majority of edges with high betweenness the discovery probability approaches one and we can reasonably expect to have a fair sampling of the network.

In most realistic samplings, however, we face a very different situation. While it is reasonable to consider ρ_T a small but finite value, the number of sources is not extensive ($N_S \sim \mathcal{O}(1)$) and their density tends to zero as N^{-1} . In this case it is more convenient to express the edge discovery probability as

$$\langle \pi_{i,j} \rangle \simeq 1 - \exp(-\epsilon \bar{b}_{ij}), \quad (10)$$

where $\epsilon = \rho_T N_S$ is the density of probes imposed to the system and the rescaled betweenness $\bar{b}_{ij} = N^{-1} b_{ij}$ is now limited in the interval $[2N^{-1}, N-1]$. In the limit of large networks $N \rightarrow \infty$ it is clear that edges with low betweenness have $\langle \pi_{i,j} \rangle \sim \mathcal{O}(N^{-1})$, for any finite value of ϵ . This readily tells us that in real situations the discovery process is generally not complete, a large part of low betweenness edges being not discovered, and that the network sampling is made progressively more accurate by increasing the density of probes ϵ .

A similar analysis can be performed for the discovery probability π_i of a vertex i . For each source-target set Ω we have that

$$\pi_i = 1 - \left(1 - \sum_{s=1}^{N_S} \delta_{i,i_s} - \sum_{t=1}^{N_T} \delta_{i,j_t}\right) \prod_{l \neq m \neq i} \left(1 - \sum_{s=1}^{N_S} \delta_{l,i_s} \sum_{t=1}^{N_T} \delta_{m,j_t} \sigma_i^{(l,m)}\right). \quad (11)$$

where $\sigma_i^{(l,m)} = 1$ if the vertex i belongs to the \mathcal{M} -path between nodes l and m , and 0 otherwise. This time it has been considered that each vertex is discovered with probability one also if it is in the set of sources and targets. The second term on the right hand side therefore expresses the probability that the vertex i does not belong to the set of sources and targets and it is not discovered by any \mathcal{M} -path between source-target pairs. By using the same *mean-field* approximation as previously, the average vertex discovery probability reads as

$$\langle \pi_i \rangle \simeq 1 - (1 - \rho_S - \rho_T) \prod_{l \neq m \neq i} \left(1 - \rho_T \rho_S \langle \sigma_i^{(l,m)} \rangle\right). \quad (12)$$

As for the case of the edge discovery probability, the average considers all possible source-target pairs weighted with probability $\rho_T \rho_S$. Also in this case, each shortest path gives a contribution $\sigma_i^{(l,m)} / \langle \sigma_i^{(l,m)} \rangle$ to $\langle \sigma_i^{(l,m)} \rangle$ for the USP and RSP models, while $\langle \sigma_i^{(l,m)} \rangle = \sigma_i^{(l,m)}$ for the ASP model. If $\rho_T \rho_S \ll 1$, by using the same approximations used to obtain Eq.(8) we obtain

$$\langle \pi_i \rangle \simeq 1 - (1 - \rho_S - \rho_T) \exp(-\rho_T \rho_S b_i), \quad (13)$$

where $b_i = \sum_{l \neq m \neq i} \langle \sigma_i^{(l,m)} \rangle$. For the USP and RSP we have that b_i is the vertex betweenness centrality that is limited in the interval $[0, N(N-1)]$ [24–26]. The betweenness value $b_i = 0$ holds for the leafs of the graph, i.e. vertices with a single edge, for which we recover $\langle \pi_i \rangle \simeq \rho_S + \rho_T$. Indeed, this kind of vertices are dangling ends discovered only if they are either a source or target themselves.

As discussed before, the most usual setup corresponds to a density $\rho_S \sim \mathcal{O}(N^{-1})$ and in the large N limit we can conveniently write

$$\langle \pi_i \rangle \simeq 1 - (1 - \rho_T) \exp(-\epsilon \bar{b}_i), \quad (14)$$

where we have neglected terms of order $\mathcal{O}(N^{-1})$ and the rescaled betweenness $\bar{b}_i = N^{-1}b_i$ is now defined in the interval $[0, N-1]$. This expression points out that the probability of vertex discovery is favored by the deployment of a finite density of targets that defines its lower bound.

We can also provide a simple approximation for the effective average degree $\langle k_i^* \rangle$ of the node i discovered by our sampling process. Each edge departing from the vertex will contribute proportionally to its discovery probability, yielding

$$\langle k_i^* \rangle = \sum_j \left(1 - \exp(-\epsilon \bar{b}_{ij}) \right) \simeq \epsilon \sum_j \bar{b}_{ij}. \quad (15)$$

The final expression is obtained for edges with $\epsilon \bar{b}_{ij} \ll 1$. In this case, the sum over all neighbors of the edge betweenness is simply related to the vertex betweenness as $\sum_j b_{ij} = 2(b_i + N - 1)$, where the factor 2 considers that each vertex path traverses two edges and the term $N - 1$ accounts for all the edge paths for which the vertex is an endpoint. This finally yields

$$\langle k_i^* \rangle \simeq 2\epsilon + 2\epsilon \bar{b}_i. \quad (16)$$

The present analysis shows that the measured quantities and statistical properties of the sampled graph strongly depend on the parameters of the experimental setup and the topology of the underlying graph. The latter dependence is exploited by the key role played by edge and vertex betweenness in the expressions characterizing the graph discovery. The betweenness is a nonlocal topological quantity whose properties change considerably depending on the kind of graph considered. This allows an intuitive understanding of the fact that graphs with diverse topological properties deliver different answers to sampling experiments.

V. NUMERICAL EXPLORATION OF GRAPHS

In this section we use the analytical results as a guidance in the discussion of extensive numerical simulations of sampling experiments in a wide range of underlying graphs derived from different models.

A. Graph models definition

In the following, we will analyze sparse undirected graphs denoted by $G = (V, E)$ where the topological

properties of a graph are fully encoded in its adjacency matrix a_{ij} , whose elements are 1 if the edge (i, j) exists, and 0 otherwise.

In particular we will consider two main classes of graphs: i) *Homogeneous graphs* in which, for large degree k , the degree distribution $P(k)$ decays exponentially or faster; ii) *Scale-free graphs* for which $P(k)$ has a heavy tail decaying as a power-law $P(k) \sim k^{-\gamma}$. Here the *homogeneity* refers to the existence of a meaningful characteristic average degree that represents the typical value in the graph. Indeed, in graphs with poissonian-like degree distribution a vast majority of vertices has degree close to the average value and deviations from the average are exponentially small in number. On the contrary, scale-free graphs are very heterogeneous with very large fluctuations of the degree, characterized by a variance of the degree distribution which diverges with the size of the network.

Another important characteristic discriminating the topology of graphs is the clustering coefficient

$$c_i = \frac{1}{k_i(k_i - 1)} \sum_{j,h} a_{ij} a_{ih} a_{jh}, \quad (17)$$

that measures the local cohesiveness of nodes. It indeed gives the fraction of connected neighbors of a given node i . The average clustering coefficient $C = \frac{1}{N} \sum_i c_i$ provides an indication of the global level of cohesiveness of the graph. The number is generally very small in random graphs that lack of correlations. In many real graphs the clustering coefficient appears to be very high and opportune models have been formulated to represent this property.

In the following we will make use of those models that can be considered prototypical examples of the various classes.

A.1 Erdős-Rényi model

The classical Erdős-Rényi (ER) model [22] for random graphs $G_{N,p}$, consists of N nodes, each edge being present in E independently with probability p . The expected number of edges is therefore $|E| = pN(N-1)/2$. In order to have sparse graphs one thus needs to have p of order $1/N$, since the average degree is $p(N-1)$. Erdős-Rényi graphs are a typical example of homogeneous graph, with degree distribution following a Poisson law, and very small clustering coefficient (of order $1/N$). Since $G_{N,p}$ can consist of more than one connected component, we consider only the largest of these components.

A.2 Watts-Strogatz model

The construction algorithm proposed by Watts and Strogatz for small-world networks [27] is the following: the

graph is initially a one-dimensional lattice of length N , with periodic boundary conditions (i.e. a ring), each vertex being connected to its $2m$ nearest neighbors (with $m > 1$). The vertices are then visited one after the other; each link connecting a vertex to one of its m nearest neighbors in the clockwise sense is left in place with probability $1 - p$, and with probability p is reconnected to a randomly chosen other vertex. Long range connections are therefore introduced. The number of edges is $|E| = Nm$, independently of p . The degree distribution has a shape similar to the case of Erdős-Rényi graphs, peaked around the average value. The clustering coefficient, however, is large if $p \ll 1$, making this network a typical example of homogeneous but clustered network. As for the ER case, it is possible to obtain graphs consisting of more than one connected component; in this case we use the largest of these components.

A.3 The Barabási-Albert model

Albert and Barabási have proposed to combine two ingredients to obtain a heterogeneous scale-free graph [28]: i) *Growth*: Starting from an initial seed of N_0 vertices connected by links, a new vertex n is added at each time step. This new site is connected to m previously existing vertices; ii) *Preferential attachment rule*: a node i is chosen by n according to the probability $P_{n \rightarrow i} = \frac{k_i}{\sum_j k_j}$; i.e. with a probability proportional to its degree. After m different vertices have been chosen to be connected to n , the growth process is iterated by introducing a new vertex, i.e. going back to step i) until the desired size of the network is reached.

This mechanism yields a connected graph of $|V| = N$ nodes with $|E| = mN$ edges. Graphs constructed with these rules have two important characteristics: the degree distribution of the nodes follow a power-law $P(k) \sim k^{-\gamma}$ with $\gamma = 3$, and the clustering coefficient is small.

A.4 Clustered and scale-free graph model

Dorogovtsev, Mendes and Samukhin have introduced in Ref. [29] a model of growing network with very large clustering coefficient C : at each time step, a new node is introduced and connected to *the two extremities of a randomly chosen edge*, thus forming a triangle. A given node is thus chosen with a probability proportional to its degree, which corresponds to the preferential attachment rule. The graphs thus obtained have N nodes, $2N$ edges, and a large clustering coefficient (≈ 0.74) along with a power-law distribution for the degree distribution of the nodes.

The main properties of the various graphs are summarized in table I: Note that the clustering is indeed large for

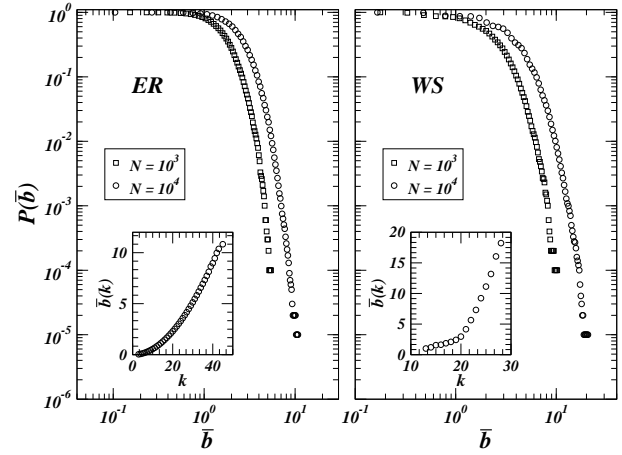


Fig. 2

CUMULATIVE DISTRIBUTION OF THE AVERAGE NODE BETWEENNESS \bar{b} IN THE ER AND WS GRAPH MODELS ($\bar{k} = 20$). THE INSET (IN LIN-LIN SCALE) SHOWS THE BEHAVIOR OF THE AVERAGE NODE BETWEENNESS AS A FUNCTION OF THE DEGREE k .

the WS and the DMS models, and that, for the scale-free models (BA and DMS), the maximum value of the connectivity (k_{max}) is much larger than the average \bar{k} .

B. Sampling homogeneous graphs

Our first set of experiments consider underlying graphs with homogeneous connectivity; namely the Erdős-Rényi (ER) and the Watts-Strogatz (WS) models. We have used networks with $N = 10^4$ nodes, $\bar{k} = 20$ unless otherwise specified; for the WS model, $p = 0.1$ has been taken. We have averaged each measurement over 10 realizations. Both models have a Poissonian degree distribution with exponential decaying tails. The distribution is therefore peaked around the average degree \bar{k} that represents the typical degree of a node. Since the topological properties governing the traceroute exploration properties is the betweenness centrality it is worth reviewing its general properties

TABLE I
MAIN CHARACTERISTICS OF THE GRAPHS USED IN THE NUMERICAL EXPLORATION.

	ER	ER	WS	BA	DMS
N	10^4	10^4	10^4	10^4	10^4
$ E $	10^5	5.10^5	10^5	4.10^4	2.10^4
\bar{k}	20	100	20	8	4
C	0.002	0.01	0.52	0.006	0.74
k_{max}	40	140	26	334	346

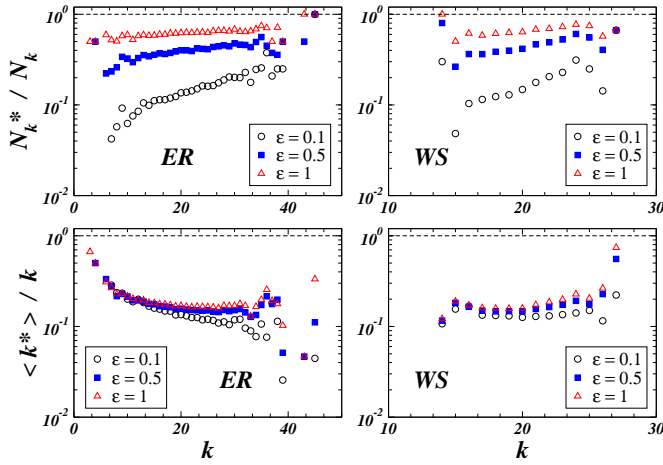


Fig. 3

FREQUENCY N_k^*/N_k OF DETECTING A VERTEX OF DEGREE k (TOP) AND PROPORTION OF DISCOVERED EDGES $\langle k^* \rangle / k$ (BOTTOM) AS A FUNCTION OF THE DEGREE IN THE ER AND WS GRAPH MODELS. THE EXPLORATION SETUP CONSIDERS $N_S = 2$ AND INCREASING PROBING LEVEL ϵ OBTAINED BY PROGRESSIVELY HIGHER DENSITY OF TARGETS ρ_T . THE y AXIS IS IN LOG SCALE TO ALLOW A FINER RESOLUTION.

in the case of the models considered here. In Fig 2 we report the vertex betweenness distribution for both the ER and WS models, confirming their poissonian distribution with an exponentially fast decaying tail. The vertex and edge betweenness are as well homogeneous quantities in these networks and their distributions are peaked around the average values \bar{b} and \bar{b}_e , respectively. These values can be considered as typical values and the betweenness distribution is narrowly distributed around these characteristic values. Moreover, on average, the betweenness is related to the degree of the vertices obtaining a $\bar{b}(k)$ that increases with the degree. On the other hand, in homogeneous graphs the range of variation in the degree is extremely limited, reverberating in small variations of the betweenness values. Finally, it must be noted that the degree and betweenness distributions do not exhibit a pronounced scaling with the size of the network because of the intrinsic exponential cut-off.

Since a large majority of vertices and edges will have a betweenness very close to the average value, we can use Eq. (10) and (14) to estimate the order of magnitude of probes that allows a fair sampling of the graph. Indeed, both $\langle \pi_{i,j} \rangle$ and $\langle \pi_i \rangle$ tend to 1 if $\epsilon \gg \max[\bar{b}^{-1}, \bar{b}_e^{-1}]$. In this limit all edges and vertices will have probability to be discovered very close to one.

At lower value of ϵ , obtained by varying ρ_T and N_S ,

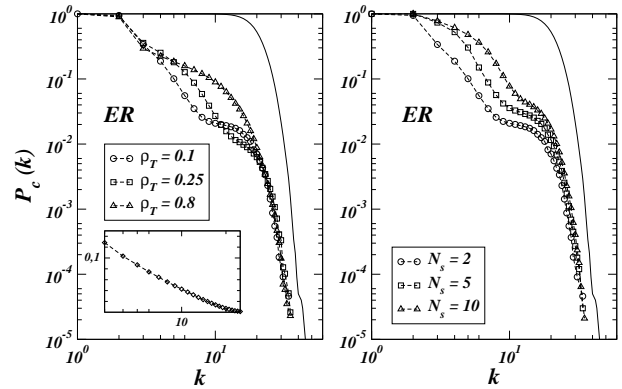


Fig. 4

CUMULATIVE DEGREE DISTRIBUTION OF THE SAMPLED ER GRAPH WITH $\bar{k} = 20$ FOR USP PROBES. THE FIGURE ON THE LEFT SHOWS SAMPLED DISTRIBUTIONS OBTAINED WITH $N_S = 2$ AND VARYING DENSITY TARGET ρ_T . IN THE INSET WE REPORT THE PECULIAR CASE $N_S = 1$ THAT PROVIDES AN APPARENT POWER-LAW BEHAVIOR WITH EXPONENT -1 AT ALL VALUES OF ρ_T . THE INSET IS IN LIN-LOG SCALE TO SHOW THE LOGARITHMIC BEHAVIOR OF THE CORRESPONDING CUMULATIVE DISTRIBUTION. THE RIGHT FIGURE SHOWS SAMPLED DISTRIBUTIONS OBTAINED WITH $\rho_T = 0.1$ AND VARYING NUMBER OF SOURCES N_S . THE SOLID LINE IS THE DEGREE DISTRIBUTION OF THE UNDERLYING GRAPH.

the underlying graph is only partially discovered. We first studied the behavior of the fraction N_k^*/N_k of discovered vertices of degree k , where N_k is the total number of vertices of degree k in the underlying graph, and the fraction of discovered edges $\langle k^* \rangle / k$ in vertices of degree k . In Fig. 3 we report the behavior of these quantities as a function of k for both the ER and WS models. The fraction N_k^*/N_k naturally increases by augmenting the density of targets and sources, and it is slightly increasing for larger degrees. The latter behavior can be easily understood by noticing that vertices with larger degree have on average a larger betweenness $b(k)$. By using Eq.(14) we have that $N_k^*/N_k \sim 1 - \exp(-\epsilon \bar{b}(k))$, obtaining the observed increase at large k . On the other hand, the range of variation of degrees in homogeneous graphs is very narrow and only a large level of probing may guarantee very large discovery probabilities. Similarly the behavior of the effective discovered degree can be understood by looking at Eq. (16) stating that $\langle k^* \rangle / k \simeq \epsilon k^{-1}(1 + \bar{b}(k))$. Indeed the initial decrease of $\langle k^* \rangle / k$ is finally compensated by the increase of $\bar{b}(k)$.

A very important quantity in the study of the statisti-

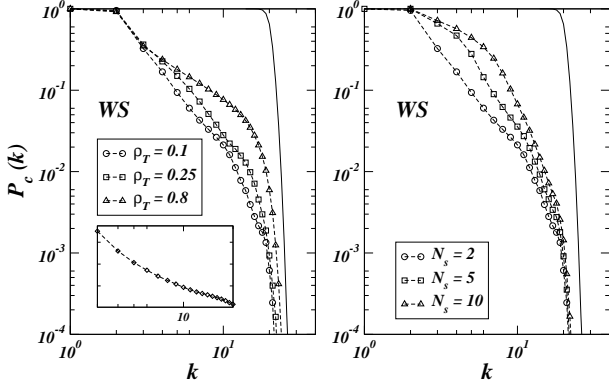


Fig. 5

CUMULATIVE DEGREE DISTRIBUTION OF THE SAMPLED WS GRAPH FOR USP PROBES. THE LEFT FIGURE SHOWS SAMPLED DISTRIBUTIONS OBTAINED WITH $N_S = 2$ AND VARYING DENSITY TARGET ρ_T . THE FIGURE ON THE RIGHT SHOWS SAMPLED DISTRIBUTIONS OBTAINED WITH $\rho_T = 0.1$ AND VARYING NUMBER OF SOURCES N_S . THE SOLID LINE IS THE DEGREE DISTRIBUTION OF THE UNDERLYING GRAPH. THE INSET SHOWS THE LOGARITHMIC BEHAVIOR OF THE CUMULATIVE DISTRIBUTION FOR $N_S = 1$ AND $\rho_T = 1$.

cal accuracy of the sampled graph is the degree distribution. In Fig. 4 we show the cumulative degree distribution $P_c(k^* > k)$ of the sampled graph defined by the ER model for increasing density of targets and sources. Sampled distributions are only approximating the genuine distribution, however, for $N_S \geq 2$ they are far from true heavy-tail distributions at any appreciable level of probing. Indeed, the distribution runs generally over a small range of degrees, with a cut-off that sets in at the average degree \bar{k} of the underlying graph. In order to stretch the distribution range, homogeneous graphs with very large average degree \bar{k} must be considered, however, other distinctive spurious effects appear in this case. In particular, since the best sampling occurs around the high degree values, the distributions develop peaks that show in the cumulative distribution as plateaus (see Fig.6). The very same behavior is obtained in the case of the WS model (see Fig. 5). Finally, in the case of RSP and ASP model, we observe that the obtained distributions are closer to the real one since they allow a larger number of discoveries.

Only in the peculiar case of $N_S = 1$ an apparent scale-free behavior with slope -1 is observed for all target densities ρ_T , as analytically shown by Clauset and Moore [8]. Also in this case, the distribution cut-off is consistently determined by the average degree \bar{k} . It is worth noting that the experimental setup with a single source is a limit case

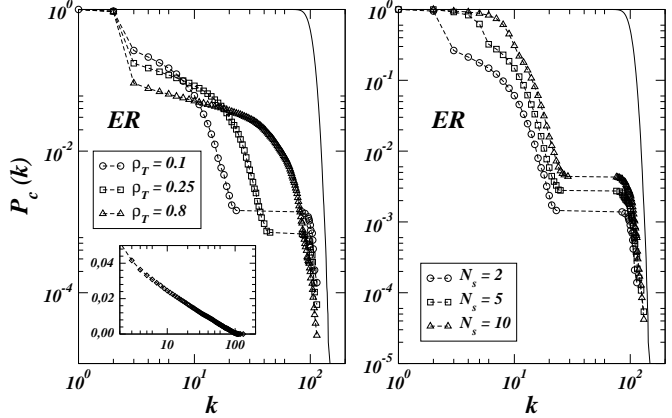


Fig. 6

CUMULATIVE DEGREE DISTRIBUTION OF THE SAMPLED ER WITH $\bar{k} = 100$. LEFT FIGURE: $N_S = 2$, AND VARIOUS VALUES OF ρ_T . THE INSET CORRESPONDS TO $N_S = 1$ AS IN FIGURE 4. RIGHT FIGURE: $\rho_T = 0.1$, VARIOUS VALUES OF N_S . IN THESE CASES THE DISTRIBUTION SHOWS THE DISTINCTIVE PRESENCE OF PLATEAUS CORRESPONDING TO THE PEAKS INDUCED BY THE SAMPLING PROCESS.

corresponding to a highly asymmetric probing process; it is therefore badly, if at all, captured by our statistical analysis which assumes homogeneous deployment.

The present analysis shows that in order to obtain a sampled graph with apparent scale-free behavior on a degree range varying over n orders of magnitude we would need the very peculiar sampling of a homogeneous underlying graph with an average degree $\bar{k} \simeq 10^n$; a rather unrealistic situation in the Internet and many other information systems where $n \geq 2$.

C. Sampling scale-free graphs

In this section, we extend the analysis made for homogeneous graphs to the case of highly heterogeneous scale-free graphs. We consider the Barabási-Albert (BA) and the Dorogovtsev, Mendes and Samukhin (DMS) graph models defined in section V-A. We have used networks of size $N = 10^4$ with $\bar{k} = 8$ for BA and $\bar{k} = 4$ for the DMS, and averaged each measurement over 10 realizations. Both models have a scale-free distribution $P(k) \sim k^{-\gamma}$ with $\gamma \simeq 3$. Moreover, the DMS model is highly clustered with an average $C \simeq 0.74$. The average degree of both models is well defined, however, the degree distribution is heavy-tailed with fluctuations diverging logarithmically with the graph size. This implies that \bar{k} is not a typical value in the network and there is an appreciable probability of finding vertices with very high degree. Analogously, the betweenness distribution is heavy-tailed, allowing for an apprecia-

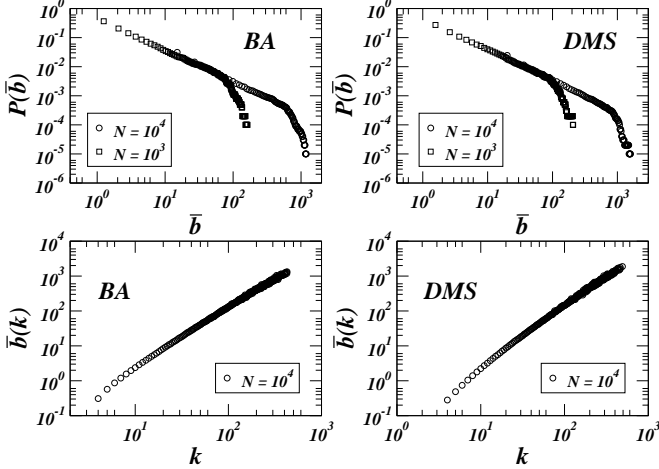


Fig. 7

CUMULATIVE DISTRIBUTION OF THE AVERAGE NODE BETWEENNESS \bar{b} (TOP) AND ITS BEHAVIOR AS A FUNCTION OF THE DEGREE k (BOTTOM) IN THE BA AND DMS GRAPH MODELS. THE PLOT IS IN LOG-LOG SCALE.

ble fraction of vertices and edges with very high betweenness [30]. In particular it is possible to show (see Fig. 7) that in scale-free graphs the site betweenness is related to the vertices degree as $\bar{b}(k) \sim k^\beta$, where β is an exponent depending on the model [30]. Since in heavy-tailed degree distributions the allowed degree is varying over several orders of magnitude, the same will occur for the betweenness values, as shown in Fig. 7. In addition, as customary for scale-free graphs, the betweenness distribution extends on a range of values that increases with the size of the network: i.e. in principle it does extend up to infinity in an infinite network.

In such a situation, even in the case of small ϵ , vertices whose betweenness is large enough ($\bar{b}(k)\epsilon \gg 1$) have $\langle \pi_i \rangle \simeq 1$. Therefore all vertices with degree $k \gg \epsilon^{-1/\beta}$ will be detected with probability one. This is clearly visible in Fig. 8 where the discovery probability N_k^*/N_k of vertices with degree k saturates to one for large degree values. Consistently, the degree value at which the curve saturates decreases with increasing ϵ . A similar effect is appearing in the measurements concerning $\langle k^* \rangle / k$. After an initial decay (see Fig. 8) the effective discovered degree is increasing with the degree of the vertices. This qualitative feature is captured by Eq. (16) that gives $\langle k^* \rangle / k \simeq \epsilon k^{-1} (1 + \bar{b}(k))$. After an initial decay the term $k^{-1} \bar{b}(k) \sim k^{\beta-1}$ takes over and the effective discovered degree approaches the real degree k .

It is evident from the previous discussions, that in scale-

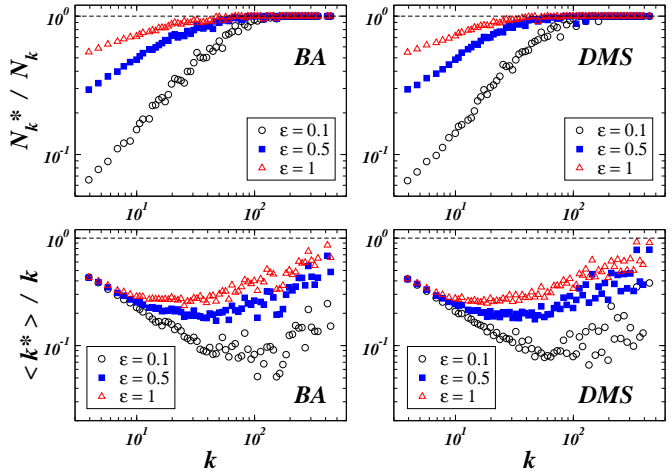


Fig. 8

FREQUENCY N_k^*/N_k OF DETECTING A VERTEX OF DEGREE k (TOP) AND PROPORTION OF DISCOVERED EDGES $\langle k^* \rangle / k$ (BOTTOM) AS A FUNCTION OF THE DEGREE IN THE BA AND DMS GRAPH MODELS. THE EXPLORATION SETUP CONSIDERS $N_S = 2$ AND INCREASING PROBING LEVEL ϵ OBTAINED BY PROGRESSIVELY HIGHER DENSITY OF TARGETS ρ_T . THE PLOT IS IN LOG-LOG SCALE TO ALLOW A FINER RESOLUTION AND ACCOUNT FOR THE WIDE VARIATION OF DEGREE IN SCALE-FREE GRAPHS.

free graphs, vertices with high degree are efficiently sampled with an effective measured degree that is rather close to the real one. This means that the degree distribution tail is fairly well sampled while deviations should be expected at lower degree values. This is indeed what we observe in numerical experiments on BA and DMS graphs (see Figs. 9 and 10). Despite both underlying graphs have a small average degree, the observed degree distribution spans more than two orders of magnitude. The distribution tail is fairly reproduced even at rather small values of ϵ . The data shows clearly that the low degree regime is instead under-sampled providing an apparent change in the exponent of the degree distribution. This effect has been noticed also by Petermann and De Los Rios in the case of single source experiments [9].

The present analysis points out that graphs with heavy-tailed degree distribution allow a better qualitative representation of their statistical features in sampling experiments. Indeed, the most important properties of these graphs are related to the heavy-tail part of the statistical distributions that are indeed well discriminated by the traceroute-like exploration.

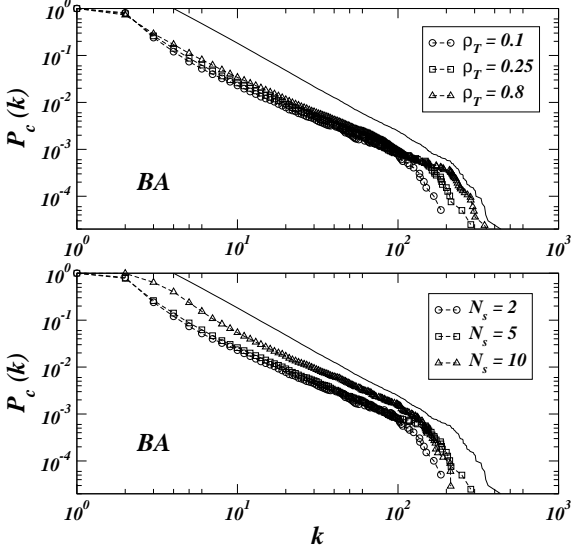


Fig. 9

CUMULATIVE DEGREE DISTRIBUTION OF THE SAMPLED BA GRAPH FOR USP PROBES. THE TOP FIGURE SHOWS SAMPLED DISTRIBUTIONS OBTAINED WITH $N_S = 2$ AND VARYING DENSITY TARGET ρ_T . THE FIGURE ON THE BOTTOM SHOWS SAMPLED DISTRIBUTIONS OBTAINED WITH $\rho_T = 0.1$ AND VARYING NUMBER OF SOURCES N_S . THE SOLID LINE IS THE DEGREE DISTRIBUTION OF THE UNDERLYING GRAPH.

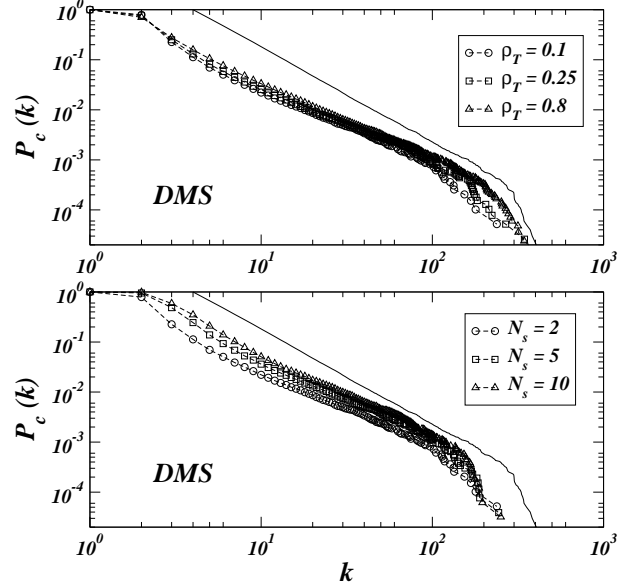


Fig. 10

CUMULATIVE DEGREE DISTRIBUTION OF THE SAMPLED DMS GRAPH FOR USP PROBES. THE TOP FIGURE SHOWS SAMPLED DISTRIBUTIONS OBTAINED WITH $N_S = 2$ AND VARYING DENSITY TARGET ρ_T . THE FIGURE ON THE BOTTOM SHOWS SAMPLED DISTRIBUTIONS OBTAINED WITH $\rho_T = 0.1$ AND VARYING NUMBER OF SOURCES N_S . THE SOLID LINE IS THE DEGREE DISTRIBUTION OF THE UNDERLYING GRAPH.

VI. OPTIMIZATION OF MAPPING STRATEGIES

In the previous sections we have shown that it is possible to have a general qualitative understanding of the efficiency of network exploration and the induced biases on the statistical properties. The quantitative analysis of the sampling strategies, however, is a much harder task that calls for a detailed study of the discovered proportion of the underlying graph and the precise deployment of sources and targets. In this perspective, very important quantities are the fraction N^*/N and E^*/E of vertices and edges discovered in the sampled graph, respectively. Unfortunately, the mean-field approximation breaks down when we aim at a quantitative representation of the results. The neglected correlations are in fact very important for the precise estimate of the various quantities of interest. For this reason we performed an extensive set of numerical explorations aimed at a fine determination of the level of sampling achieved for different experimental setups.

In Fig. 11 we report the proportion of discovered edges in the numerical exploration of the graph models defined previously for increasing level of probing ϵ . The level of probing is increased either by raising the number of sources at fixed target density or by raising the target den-

sity at fixed number of sources. As expected, both strategies are progressively more efficient with increasing levels of probing. In scale-free graphs, it is also possible to see that when the number of sources is $N_S \sim \mathcal{O}(1)$ the increase of the number of targets achieves better sampling than increasing the deployed sources. On the other hand, it is easy to perceive that the shortest path route mapping is a symmetric process if we exchange sources with targets. This is confirmed by numerical experiments in which we use a very large number of sources and a number of targets $\rho_T \sim \mathcal{O}(1/N)$, where the trends are opposite: the increase of the number of sources achieves better sampling than increasing the deployed targets.

This finding hints toward a behavior that is determined by the number of sources and targets, N_S and N_T . Any quantity is thus a function of N_S and N_T , or equivalently of N_S and ρ_T . This point is clearly illustrated in Fig. 12 and 13, where we report the behavior of E^*/E and N^*/N at fixed ϵ and varying N_S and ρ_T . The curves exhibit a non-trivial behavior and since we will work at fixed $\epsilon = \rho_T N_S$, any measured quantity can then be written as $f(\rho_T, \epsilon/\rho_T) = g_\epsilon(\rho_T)$. Very interestingly, the curves

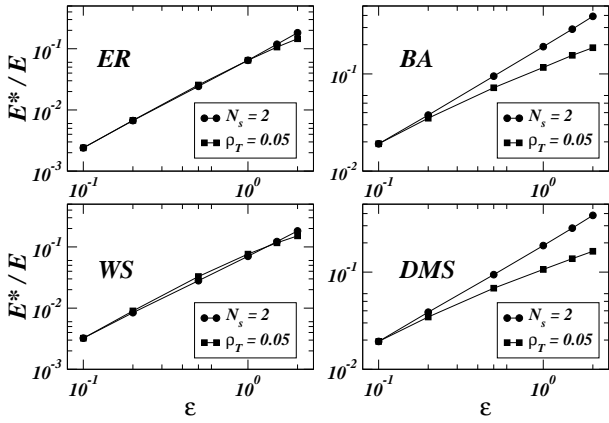


Fig. 11

BEHAVIOR OF THE FRACTION OF DISCOVERED EDGES IN EXPLORATIONS WITH INCREASING ϵ . FOR EACH UNDERLYING GRAPH STUDIED WE REPORT TWO CURVES CORRESPONDING TO LARGER ϵ ACHIEVED BY INCREASING THE TARGET DENSITY ρ_T AT $N_S = 2$ OR THE NUMBER OF SOURCES N_S AT $\rho_T = 0.05$.

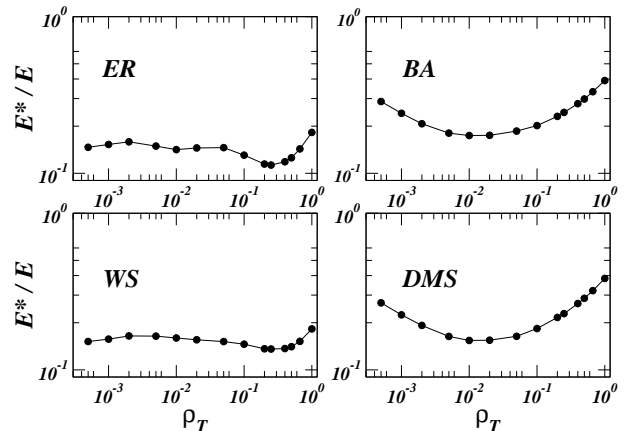


Fig. 12

BEHAVIOR AS A FUNCTION OF ρ_T OF THE FRACTION OF DISCOVERED EDGES IN EXPLORATIONS WITH FIXED ϵ (HERE $\epsilon = 2$). SINCE $\epsilon = \rho_T N_S$, THE INCREASE OF ρ_T CORRESPONDS TO A LOWERING OF THE NUMBER OF SOURCES N_S .

show a structure allowing for local minima and maxima in the discovered portion of the underlying graph.

This feature can be explained by a simple symmetry argument. The model for traceroute is symmetric by the exchange of sources and targets, which are the endpoints of shortest paths: an exploration with $(N_T, N_S) = (N_1, N_2)$ is equivalent to one with $(N_T, N_S) = (N_2, N_1)$. In other words, at fixed $\epsilon = N_1 N_2 / N$, a density of targets $\rho_T = N_1 / N$ is equivalent to a density $\rho'_T = N_2 / N$. Since $N_2 = \epsilon / \rho_T$ we obtain that at constant ϵ , experiments with ρ_T and $\rho'_T = \epsilon / (N \rho_T)$ are equivalent obtaining by symmetry that any measured quantity obeys the equality

$$g_\epsilon(\rho_T) = g_\epsilon \left(\frac{\epsilon}{N \rho_T} \right). \quad (18)$$

This equation implies a symmetry point signaling the presence of a maximum or a minimum at $\rho_T = \epsilon / (N \rho_T)$. We therefore expect the occurrence of a symmetry in the graphs of Fig.12 at $\rho_T \simeq \sqrt{\epsilon / N}$. Indeed, the symmetry point is clearly visible and in quantitative good agreement with the previous estimate in the case of scale-free graphs. On the contrary, homogeneous underlying topology have a smooth behavior that makes difficult the clear identification of the symmetry point. It must be also noticed that USP probes create a certain level of correlations in the exploration that tends to hide the complete symmetry of the curves.

The previous results imply that at fixed levels of probing ϵ different proportions of sources and targets may achieve

different levels of sampling. This hints to the search for optimal strategies in the relative deployment of sources and targets. The picture, however, is more complicated if we look at other quantities in the sampled graph. In Fig.14 we show the behavior at fixed ϵ of the average degree \bar{k}^* measured in sampled graphs normalized with the actual average degree \bar{k} of the underlying graph as a function of ρ_T . The plot shows also in this case a symmetric structure with a maximum at the symmetry point. By comparing Fig.14 with Fig.12 we notice that the symmetry point is of a different nature for different quantities. Hence, where we have a minimum in the fraction of discovered edges, we have the best estimate of the average degree. This implies that at the symmetry point the exploration discovers less edges than in other setups, however, achieving a more efficient sampling of the effective degree for the discovered vertices. A similar problem is obtained by studying the behavior of the ratio C^*/C between the clustering coefficient of the sampled and the underlying graphs. We studied this quantity for the WS and DMS models that have a high clustering level. Also in these cases, as shown in Fig.15, the best level of sampling is achieved at particular values of ϵ and N_S that are conflicting with the best sampling of other quantities.

The evidence purported in this section hints to a possible optimization of the sampling strategy. The optimal solution, however, appears as a trade-off strategy between the different level of efficiency achieved in competing ranges

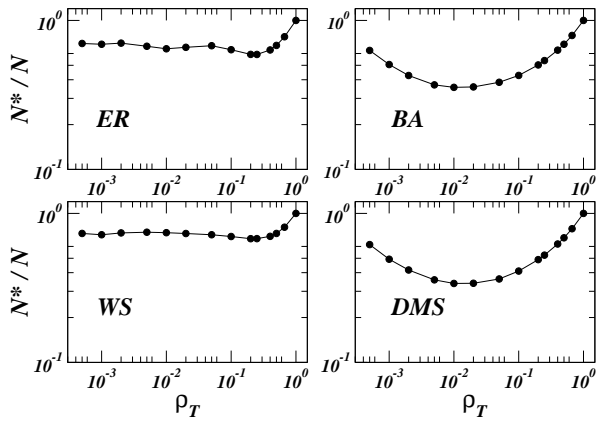


Fig. 13

BEHAVIOR AS A FUNCTION OF ρ_T OF THE FRACTION OF DISCOVERED NODES IN EXPLORATIONS WITH FIXED ϵ

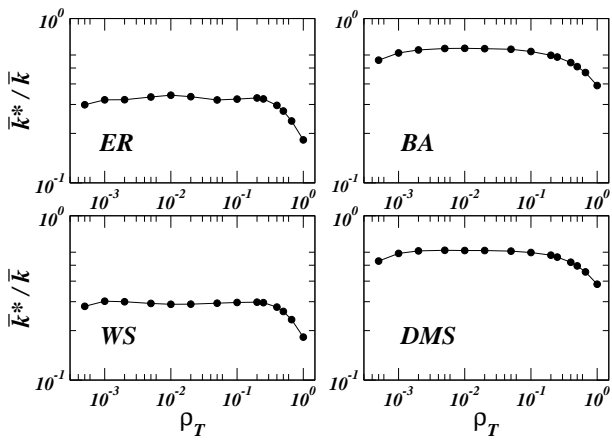


Fig. 14

BEHAVIOR AS A FUNCTION OF ρ_T OF THE FRACTION OF THE NORMALIZED AVERAGE DEGREE \bar{k}^*/\bar{k} FOR A FIXED PROBING LEVEL ϵ (HERE $\epsilon = 2$).

of the experimental setup. In this respect, a detailed and quantitative investigation of the various quantities of interest in different experimental setups is needed in order to pinpoint the most efficient deployment of source-target pairs depending on the underlying graph topology.

VII. CONCLUSIONS AND OUTLOOK

The rationalization of the exploration biases at the statistical level provides a general interpretative framework for the results obtained from the numerical experiments on

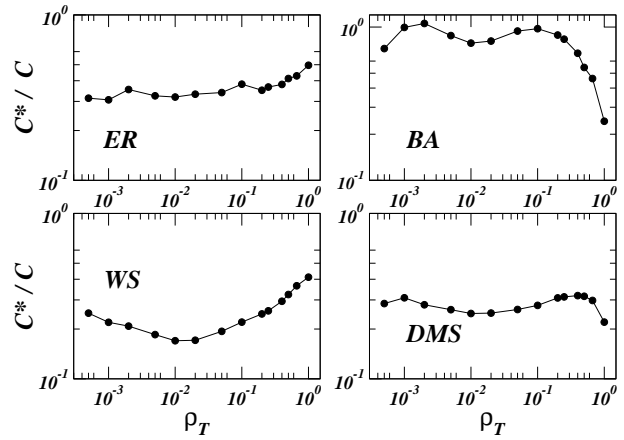


Fig. 15

BEHAVIOR AS A FUNCTION OF ρ_T OF THE FRACTION OF THE NORMALIZED AVERAGE CLUSTERING COEFFICIENT C^*/C FOR A FIXED PROBING LEVEL ϵ (HERE $\epsilon = 2$).

graph models. The sampled graph clearly distinguishes the two situations defined by homogeneous and heavy-tailed topologies, respectively. This is due to the exploration process that statistically focuses on high betweenness nodes, thus providing a very accurate sampling of the distribution tail. In graphs with heavy-tails, such as scale-free networks, the main topological features are therefore easily discriminated since the relevant statistical information is encapsulated in the degree distribution tail which is fairly well captured. Quite surprisingly, the sampling of homogeneous graphs appears more cumbersome than those of heavy-tailed graphs. Dramatic effects such as the existence of apparent power-laws, however, are found only in very peculiar cases. In general, exploration strategies provide sampled distributions with enough signatures to distinguish at the statistical level between graphs with different topologies.

This evidence might be relevant in the discussion of real data from Internet mapping projects. Indeed, data available so far indicate the presence of heavy-tailed degree distribution both at the router and AS level. In the light of the present discussion, it is very unlikely that this feature is just an artifact of the mapping strategies. The upper degree cut-off at the router and AS level runs up to 10^2 and 10^3 , respectively. A homogeneous graph should have an average degree comparable to the measured cut-off and this is hardly conceivable in a realistic perspective (for instance, it would require that nine routers over ten would have more than 100 links to other routers). In addition, the major part of mapping projects are multi-source, a feature that we have shown to readily wash out the presence

of spurious power-law behavior. On the contrary, power-law tails are easily sampled with particular accuracy for the large degree part, generally at all probing levels. This makes very plausible, and a natural consequence, that the heavy-tail behavior observed in real mapping experiments is a genuine feature of the Internet.

On the other hand, it is important to stress that while at the qualitative level the sampled graphs allow a good discrimination of the statistical properties, at the quantitative level they might exhibit considerable deviations from the true values such as average degree, distribution exponent and clustering properties. In this respect, it is of major importance to define strategies that optimize the estimate of the various parameters and quantities of the underlying graph. In this paper we have shown that the proportion of sources and targets may impact on the accuracy of the measurements even if the number of total probes imposed to the system is the same. For instance, the deployment of a highly distributed infrastructure of sources probing a limited number of targets may result as efficient as a few very powerful sources probing a large fraction of the addressable space. The optimization of large network sampling is therefore an open problem that calls for further work aimed at a more quantitative assessment of the mapping strategies both on the analytic and numerical side.

ACKNOWLEDGMENTS

We are grateful to M. Crovella, P. De Los Rios, T. Erlebach, T. Friedman, M. Latapy and T. Petermann for very useful discussion and comments. This work has been partially supported by the European Commission Fet-Open project COSIN IST-2001-33555 and contract 001907 (DELIS).

REFERENCES

- [1] The National Laboratory for Applied Network Research (NLANR), sponsored by the National Science Foundation. (see <http://moat.nlanr.net/>).
- [2] The Cooperative Association for Internet Data Analysis (CAIDA), located at the San Diego Supercomputer Center. (see <http://www.caida.org/home/>).
- [3] Topology project, Electric Engineering and Computer Science Department, University of Michigan (<http://topology.eecs.umich.edu/>).
- [4] SCAN project at the Information Sciences Institute (<http://www.isi.edu/div7/scan/>).
- [5] Internet mapping project at Lucent Bell Labs (<http://www.cs.bell-labs.com/who/ches/map/>).
- [6] M. Faloutsos, P. Faloutsos, and C. Faloutsos, "On Power-law Relationships of the Internet Topology," *ACM SIGCOMM '99, Comput. Commun. Rev.* **29**, 251–262 (1999).
- [7] A. Lakhina, J. W. Byers, M. Crovella and P. Xie, "Sampling Biases in IP Topology Measurements," Technical Report BUCS-TR-2002-021, Department of Computer Sciences, Boston University (2002).
- [8] A. Clauset and C. Moore, "Traceroute sampling makes random graphs appear to have power law degree distributions," *arXiv:cond-mat/0312674* (2003).
- [9] T. Petermann and P. De Los Rios, "Exploration of Scale-Free Networks," *arXiv:cond-mat/0401065* (2004).
- [10] R. Govindan and H. Tangmunarunkit, "Heuristics for Internet Map Discovery," *Proc. of IEEE Infocom 2000, Volume 3*, IEEE Computer Society Press, 1371–1380, (2000).
- [11] A. Broido and K. C. Claffy, "Internet topology: connectivity of IP graphs," *San Diego Proceedings of SPIE International symposium on Convergence of IT and Communication*. Denver, CO. 2001
- [12] G. Caldarelli, R. Marchetti, and L. Pietronero, "The Fractal Properties of Internet," *Europhys. Lett.* **52**, 386 (2000).
- [13] R. Pastor-Satorras, A. Vázquez, and A. Vespignani, "Dynamical and Correlation Properties of the Internet," *Phys. Rev. Lett.* **87**, 258701 (2001); A. Vázquez, R. Pastor-Satorras, and A. Vespignani, "Large-scale topological and dynamical properties of the Internet," *Phys. Rev. E* **.65**, 066130 (2002).
- [14] Q. Chen, H. Chang, R. Govindan, S. Jamin, S. J. Shenker, and W. Willinger, "The Origin of Power Laws in Internet Topologies Revisited," *Proceedings of IEEE Infocom 2002*, New York, USA.
- [15] A. Medina and I. Matta, "BRITE: a flexible generator of Internet topologies," *Tech. Rep. BU-CS-TR-2000-005*, Boston University, 2000.
- [16] C. Jin, Q. Chen, and S. Jamin, "INET: Internet topology generators," *Tech. Rep. CSE-TR-433-00*, EECS Dept., University of Michigan, 2000.
- [17] S. N. Dorogovtsev and J. F. F. Mendes, *Evolution of networks: From biological nets to the Internet and WWW* (Oxford University Press, Oxford, 2003).
- [18] P. Baldi, P. Frasconi and P. Smyth, *Modeling the Internet and the Web: Probabilistic methods and algorithms* (Wiley, Chichester, 2003).
- [19] R. Pastor-Satorras and A. Vespignani, *Evolution and structure of the Internet: A statistical physics approach* (Cambridge University Press, Cambridge, 2004).
- [20] H. Burch and B. Cheswick, "Mapping the internet," *IEEE computer*, **32**(4), 97–98 (1999).
- [21] W. Willinger, R. Govindan, S. Jamin, V. Paxson, and S. Shenker, "Scaling phenomena in the Internet: Critically examining criticality," *Proc. Natl. Acad. Sci USA* **99** 2573–2580, (2002).
- [22] P. Erdős and P. Rényi, "On random graphs I," *Publ. Math. Inst. Hung. Acad. Sci.* **5**, 17 (1960).
- [23] J.-L. Guillaume and M. Latapy, "Relevance of Massively Distributed Explorations of the Internet Topology: Simulation Results," (2004).
- [24] L. C. Freeman, "A Set of Measures of Centrality Based on Betweenness," *Sociometry* **40**, 35–41 (1977).
- [25] U. Brandes, "A Faster Algorithm for Betweenness Centrality," *J. Math. Soc.* **25**(2), 163–177, (2001).
- [26] K.-I. Goh, B. Kahng, and D. Kim, "Universal Behavior of Load Distribution in Scale-Free Networks," *Phys. Rev. Lett.* **87**, 278701 (2001).
- [27] D. J. Watts and S. H. Strogatz, "Collective dynamics of small-world networks," *Nature* **393**, 440–442 (1998).
- [28] A.-L. Barabási and R. Albert, "Emergence of scaling in random networks," *Science* **286**, 509–512 (1999).
- [29] S. N. Dorogovtsev, J. F. F. Mendes, and A. N. Samukhin, "Size-dependent degree distribution of a scale-free growing network," *Phys. Rev. E* **63**, 062101 (2001)

[30] M. Barthélemy, “Betweenness Centrality in Large Complex Networks,” *Eur. Phys. J B* **38**, 163 (2004).